IEEE Access
Multidisciplinary ⋮ Rapid Review ⋮ Open Access Journal

Received 19 February 2023, accepted 1 April 2023, date of publication 5 April 2023, date of current version 12 April 2023.

*Digital Object Identifier 10.1109/ACCESS.2023.3264900*

RESEARCH ARTICLE

# Effect of Rear Contact Coverage and Improvement of Efficiency of Crystalline p-Si Solar Cell Compared to State of Art PERC Cell

**S. BANERJEE[1], S. S. A. ASKARI[2], (Member, IEEE), AND M. K. DAS[3], (Senior Member, IEEE)**

[1]Department of Electronics and Communication Engineering, NSHM Institute of Engineering and Technology, Durgapur, West Bengal 713212, India
[2]Department of Electronics Engineering, IIT(ISM) Dhanbad, Dhanbad, Jharkhand 826004, India
[3]Centre of Excellence in Renewable Energy (CERE), Department of Electronics Engineering, IIT(ISM) Dhanbad, Dhanbad, Jharkhand 826004, India

Corresponding author: M. K. Das (mukulkdas@iitism.ac.in)

This work was supported by the Ministry of Human Resource Development (MHRD), Government of India, through the Project "Establishment of Centers of Excellence in Renewable Energy," Indian Institute of Technology (IIT) [Indian School of Mines (ISM)] Dhanbad, Dhanbad, India, in 2014, under Grant 5-6/2013-TS-VII.

**ABSTRACT** A device simulation model for localized contact rear side oxide-passivated solar cell has been developed to study the effects of rear contact coverage and fixed charge density dependent field-effect passivation on the performance of *p*-Si solar cell. Models describing hetero-interface physics related to metal-semiconductor, metal-oxide-semiconductor junctions and interface recombination are considered in the simulation, results of which are verified with the reported experimental data. A detailed analysis of the effect of surface passivation is presented and an analytical design with optimized set of parameters is outlined for fabricating the cell. The result shows that the efficiency of the solar cell can be substantially enhanced by controlling parameters mainly the ratio between localized back contact to the non-contact area and the fixed charge density at the oxide-interface. A maximum efficiency of ∼25% for a crystalline *p*-Si solar cell with a comparatively lower lifetime can be obtained by a suitable choice of the design parameters with an added suitable choice of doping concentration in the emitter and absorber and the oxide layer thickness.

**INDEX TERMS** $Al_2O_3$, crystalline silicon, local contact, numerical modeling, solar cell, surface passivation.

## I. INTRODUCTION

The photovoltaic industry is dominated by crystalline silicon (*c*-Si) where 90% of the market is based on full-area aluminium back surface field (Al-BSF) technology. However, the standard *c*-Si solar cell is in transition from a full-area Al-BSF to passivated emitter rear cell (PERC) structure with localized back contact [1]. The key problem of the full-area Al-BSF includes moderate passivation at rear surface and poor internal reflectivity of the infrared lights. These internal reflectivity and limited passivation can be improved by rear passivated cells [2], [3]. Rear surface passivation of c-Si solar cell is exhibited by oxide film, such as silicon dioxide ($SiO_2$) or aluminium oxide ($Al_2O_3$) [4], [5], [6]. Oxide material is chosen mainly because of its capability of field-effect passivation by its underlying fixed charges as well as chemical passivation [7], [8]. In case of tunnel oxide passivated rear surface Si-solar cell with full area contact, a very thin oxide (*e.g.*, $SiO_2$ for *n*-Si wafer) layer is deposited at the bottom of the absorber layer [4], [9]. However, thickness of oxide layer needs to be restricted to few nanometers (∼1.5 nm – 3 nm) in this case to ensure the tunneling [4], [6], [10]. Deposition of ultrathin oxide layer is mostly done by Atomic Layer Deposition (ALD) which suffers from very slow deposition rate (2 nm/min) and high processing cost [5], [9], [11], [12]. Instead of passivation by tunnel oxide, Rauer et al. and Black and McIntosh, used a comparatively thicker oxide ($Al_2O_3$) with localized contact regions for rear surface passivation of *p*-Si solar cell [13], [14]. However, in case of thick-oxide passivated rear surface with localized contact structure, carriers need to travel more resistive path to reach the back-electrode. Wider localized contact would reduce the resistive loss but at the cost of lesser passivation. Also, the doping concentration of the absorber layer has an

The associate editor coordinating the review of this manuscript and approving it for publication was Guangcun Shan.

important role on the resistive and bulk recombination loss. Therefore, design of the device, primarily in terms of rear contact coverage *i.e.* ratio between contact and non-contact surface area and absorber doping concentration are important.

Current PERC cells provide average power conversion efficiency of 22-23% [14], [15]. However, high efficient lab scale PERC cell uses bulk *p*-Si wafer having lifetime higher than 1.5 ms, which is very expensive for mass production [16]. Our design objective is to achieve higher efficiency of low carrier-lifetime p-Si wafer, incorporating localized rear contact passivated structure and to address the effect of rear contact to non-contact area ratio. It is evident that by choosing proper contact to non-contact area ratio and underlying fixed charge density of passivation layer, optimization of the cell is possible. Therefore, present work focuses on the effect of the localized contact to non-contact area fraction and design of high efficient *p*-Si solar cell by optimizing the passivation layer parameters and doping concentration of base and emitter using ATLAS, the SILVACO-TCAD simulator.

Key significance of physical device modeling includes more physics insights of the structure, use of realistic parameters and most importantly reduction in development cost and fabrication time [17], [18]. Noteworthy to mention, simulation included the physical parameters and models related to the optical and electrical properties of metal-semiconductor, metal-oxide-semiconductor and semiconductor-semiconductor interfaces along with the property of bulk Si-absorber. The model is verified with the reported experimental result for similar-most structure. Effect of oxide-thickness dependent fixed charge density on the surface recombination velocity and hence on the performance of the device has also been investigated.

## II. DEVICE STRUCTURE AND SIMULATION MODELS

The cross-sectional view of the device structure, considered in this work, is shown in Fig. 1(a). A *p*-type planer *Cz*-Si wafer and $n^+$ doped thin layer (0.4 $\mu$m) are considered to be the absorber and emitter layers respectively. A thick ($\sim$20 nm – 30 nm) $Al_2O_3$ at the bottom of Si-absorber is considered to act as passivating layer. Aluminum-made equi-spaced and equi-wide selective regions at the bottom of Si-absorber are considered to act as localized contacts which are connected to the back Al-electrode as shown by yellow color in Fig. 1(a). Use of conventional Al-paste through local opening or punch-through of back-electrode material by LASER-assisted selective point/line annealing may be considered as feasible techniques for formation of these localized contacts [13]. During formation of localized contacts by either of the methods, a thin $p^+$ Al-Si eutectic layer is formed on top of the localized contacts, as shown in the figure. This may serve as back surface field for localized contacts. Band diagrams of the proposed structure along two cut-lines, AB (passing through localized contact) and CD (passing through oxide layer) are shown in Fig. 1(b) and (c) respectively. Since the formation of $p^+$ layer is of amorphous in nature, thus band gap is higher compared to bulk *c*-Si,

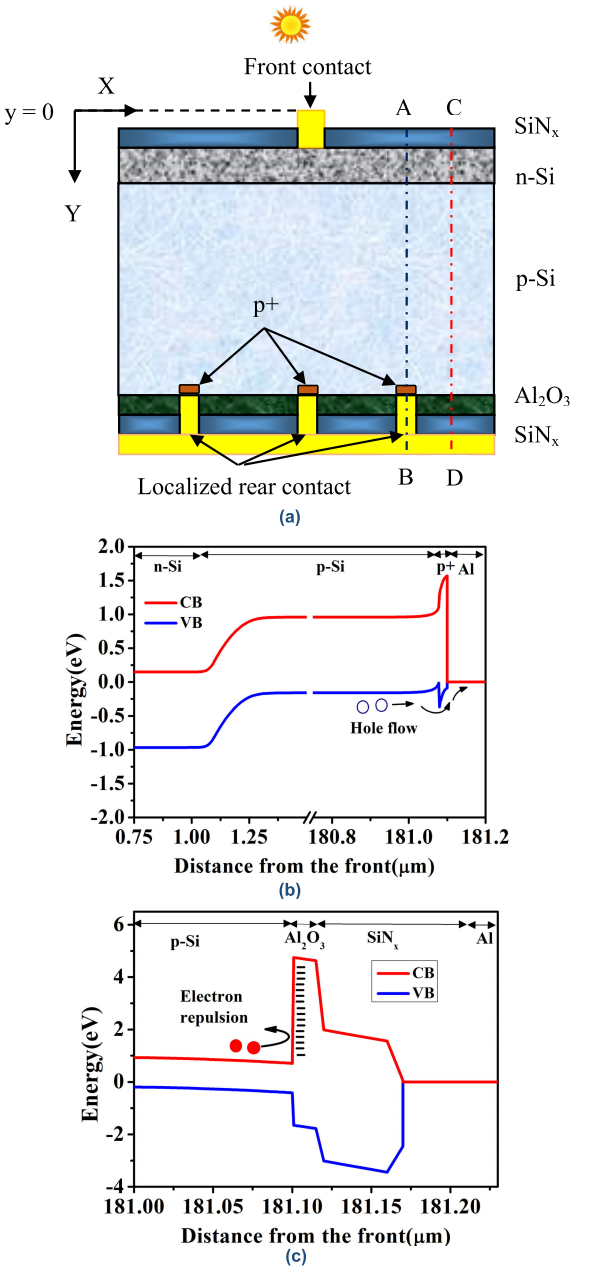


**FIGURE 1.** Schematic structure of thick-oxide passivated *p*-Si solar cell with localized rear contact; (b) Equilibrium energy-band diagrams along cut-lines, AB [through localized contact] and (c) along cutline CD [through non-contact region]. Red solid dots represent electrons and blue hollow dots represent holes.

which is visible on Fig. 1(b). Excess minority electrons in *p*-Si absorber cannot pass through the oxide barrier. Rather, they are repelled back by the underlying negative fixed charges as shown in Fig. 1(c): CD-cutline curve. Thus, recombination of electrons at the back-surface of *p*-Si absorber is reduced and hence field effect passivation is achieved. However, holes are supposed to reach the rear-electrode through localized contacts.

In order to include the effect of bulk and surface recombination in simulation, Shockley-Read-Hall (SRH) model with necessary reforms is taken account [19]. For

bulk recombination, single defect state at the middle of the forbidden gap is considered and the effect of impurity concentration on carrier life-time is included through concentration dependent SRH model in TCAD simulation. However, recombination at the interface between different layers is more significant compared to the bulk recombination for the device structure considered in this work. To include the effect of interface recombination at the metal-semiconductor interface in particular, associated model for effective lifetime ($\tau^{\mathbf{eff}}$), as per the following expression, is taken account in the simulation.

$$\frac{1}{\tau_n^{eff}} = \frac{1}{\tau_n^b} + \frac{d}{A}Sn \tag{1}$$

$$\frac{1}{\tau_p^{eff}} = \frac{1}{\tau_p^b} + \frac{d}{A}Sp \tag{2}$$

where, $\tau_n^b(\tau_p^b)$ is bulk lifetime of electron(hole), $d$ is characteristics diffusion length at interface, $A$ is the area at the interface and $S_n(S_p)$ is surface recombination velocity(SRV) of electron(hole). Carrier lifetime for highly doped silicon is affected by auger recombination, which is included in the model.

Interface defect density, carrier capture cross-section and thermal velocity dependent interface ($p$-Si/oxide) recombination velocity are also considered in the simulation [20]. Effect of underlying negative fixed charges of $Al_2O_3$ is included through alteration of charge density in Poisson's equation, which ultimately modifies the electric field at the interface and hence motion of carriers. Moreover, these fixed charges are responsible for reduced recombination rate at the oxide interface since they decrease surface recombination velocity of minority carriers. Additionally, the contact resistance is included by taking account the junction between localized contact (with BSF layer) and $p$-Si absorber as Schottky type.

Now, the chemical passivation effect is taken account in the simulation by changing the interface defect density at metal/semiconductor interface. Effect of electric field passivation due to negative fixed charge at the $Al_2O_3/p$-Si interface is considered through self-consistent solution of Poisson's equation and continuity equation for drift-diffusion model in TCAD simulation. Here in SRH model, the surface recombination rate is converted into volume recombination rate by dividing it with characteristic diffusion length. This small length is considered as thickness across the recombination zone within the interface of semiconductor/insulator. Traps are located near the interface between two different materials within this thin length. Recombination zone is located next to interface with highest minority carrier density [21]. Model for electric field dependent mobility of carriers takes care of the effect of electric field at the interface. Concentration dependent mobility and carrier scattering effect have also been included in the simulation model for higher carrier concentration at emitter layer. Model associated with barrier lowering effect at Schottky contact has been considered to include the effect of contact resistances.

**TABLE 1. Some important structural and material parameters considered in the simulation.**

| Material and device parameters | Value |
|---|---|
| Thickness of absorber layer($p$-Si) | 180 µm |
| Thickness of emitter layer(n-Si) | 0.4 µm [30] |
| Thickness of $Al_2O_3$ | 20 nm(varied) [14] |
| Thickness of $SiN_x$ | 90 nm [23,24] |
| Doping density of absorber | $2\times10^{16}$ cm$^{-3}$ (varied) [9,24,25] |
| Doping density of emitter | $1\times10^{17}$ cm$^{-3}$ (varied) [21] |
| Interface fixed charge density of $Al_2O_3$ | $10^{11}$ cm$^{-2}$(varied)[20] |
| SRV at Si/ $Al_2O_3$ interface | 10 cm/s [20] |
| SRV at Si/ Al interface | $10^7$ cm/s [30] |
| Bulk lifetime | 1 ms [20,25] |

**TABLE 2. Some experimental (reported) and simulated performance parameters for comparison.**

| Type of Solar Cell | $J_{SC}$ (mA/cm$^2$) | | $V_{OC}$ (mV) | | $FF$ (%) | | $\eta$ (%) | |
|---|---|---|---|---|---|---|---|---|
| | *Sim.* | *Exp.* | *Sim.* | *Exp.* | *Sim.* | *Exp.* | *Sim.* | *Exp.* |
| Oxide passivated ($Al_2O_3/SiN_x$ stack) $p$-Si-solar cell [23] | 39.9 | 39.9 | 654 | 656 | 81.2 | 81.1 | 21.4 | 21.3 |
| Non-passivated $p$-Si-solar cell [22] | 33.1 | 33.4 | 575 | 583 | 79.4 | 78 | 15.2 | 15.2 |

## III. DESIGN AND ANALYSIS OF RESULTS

Reference structures of un-passivated (with BSF) and thick-oxide passivated $p$-Si solar cell have been modeled and developed model is verified with reported experimental result of un-passivated structure [22] and oxide passivated structure [23] respectively. For the verification, simulation is carried out based on the available values of material and device parameters in literatures [9], [14], [20], [21], [22], [23], [24], [25], [30].

Some important material and device parameters are presented in Table 1. Absorber is considered to be 0.5 Ω-cm p-type $Cz$-Si wafer. Surface state density of $p$-Si is in the order of $10^{12}$ cm$^{-2}$ [26]. In the simulation, both acceptor as well as donor like traps have been considered. These traps are considered to be deep traps with electron and hole capture cross section of $10^{-15}$ cm$^{-2}$ and $10^{-16}$ cm$^{-2}$ respectively at the interface of bulk silicon and oxide. Capture cross sections for the free carriers are treated as constant for all energies. The spatial distribution of the interface states is considered to be uniform on the semiconductor surface [27]. In-line with the experimentally reported structure, a capping layer of $SiN_x$ (90 nm) is also considered [23], [24]. It may be mentioned here that, $SiN_x$ does not have much impact on field effect passivation rather it provides stability during annealing of rear contact. Ratio between the widths of localized contact and non-contact regions is assumed to be ∼0.05.

Comparison of simulated and experimental results, in terms of short circuit current density ($J_{SC}$), open circuit voltage ($V_{OC}$), fill factor ($FF$) and efficiency ($\eta$) are presented in Table 2. Results show a close agreement of

**TABLE 3. Performance parameters upon variation of SRV at metal/semiconductor interface for the reference cell.**

| Surface recombination velocity(cm/s) | $J_{SC}$ (mA/cm$^2$) | $V_{OC}$ (mV) | $FF$ (%) | $\eta$ (%) |
|---|---|---|---|---|
| $10^5$ | *40.08* | *0.661* | *81.38* | *21.73* |
| $10^6$ | *40.06* | *0.660* | *81.33* | *21.68* |
| $10^7$ | *39.92* | *0.654* | *81.17* | *21.37* |
| $10^8$ | *39.52* | *0.625* | *79.79* | *19.86* |

simulated result with the experimental data. Although the result of the cell under consideration is found with fixed surface recombination velocity as reported in the literature at metal/semiconductor interface [30], however the surface recombination velocity may vary due to contamination, gas flow while formation of passivation layer etc. Therefore, the effect of variation of surface recombination velocities is also studied and result is shown in Table 3. It is evident that both efficiency and fill-factor decrease upto the range of $10^7$ cm/s and degrade drastically after SRV$>10^7$ cm/s. However due to the presence of highly doped layer at the interface of metal and semiconductor both for top and bottom contact, SRV beyond $10^7$ cm/s won't be practicable.

Based on the verified model, performance of thick-oxide-passivated solar cell with localized contacts is analyzed as follows. Material and device parameters are kept fixed as mentioned earlier, except if they are varied to observe the effect of their variation. Throughout the analysis, solar spectrum of AM1.5G standard is used and the bulk lifetime of $p$-Si absorber is taken as 1 ms considering the injection level (emitter doping) at higher side [20], [25].

For thick-oxide passivated structure, current is supposed to flow through localized contacts unlike the case of tunnel-oxide passivated structure where the current can flow through ultra-thin-oxide layer to reach at the back-electrode. To confirm this, TCAD-simulated current flow lines for two different structures, tunnel oxide(ultra-thin) passivated with full area back contact and thick-oxide passivated with localized contact are shown in Fig. 2. It shows that the carriers need to propagate longer path, which yields more resistive as well as recombination loss in thick-oxide passivated solar cell. This can be minimized by increasing width of the localized contact regions. But it may result deterioration of surface passivation. So, for optimum design of width, let us analyze the effect of ratio ($R$) between localized contact to non-contact area on the performance of the device. Variation of $J_{SC}$ and $\eta$ with the ratio between total contact region width and total non-contact region width for different absorber doping concentrations is shown in Fig. 3(a). The ratio between area of contact region to area of non-contact regions turns out to be the ratio of their widths (along X-axis) since the regions are considered to be extended continuously along the breadth (say Z-axis) of the device.

It is observed that $J_{SC}$, $V_{OC}$ and $\eta$ decreases non-linearly with increasing the ratio beyond $\sim$0.05, irrespective of absorber doping concentration. The non-linear variation of $\eta$is mainly caused by the $J_{SC}$ as well as $V_{OC}$ variation with $R$.

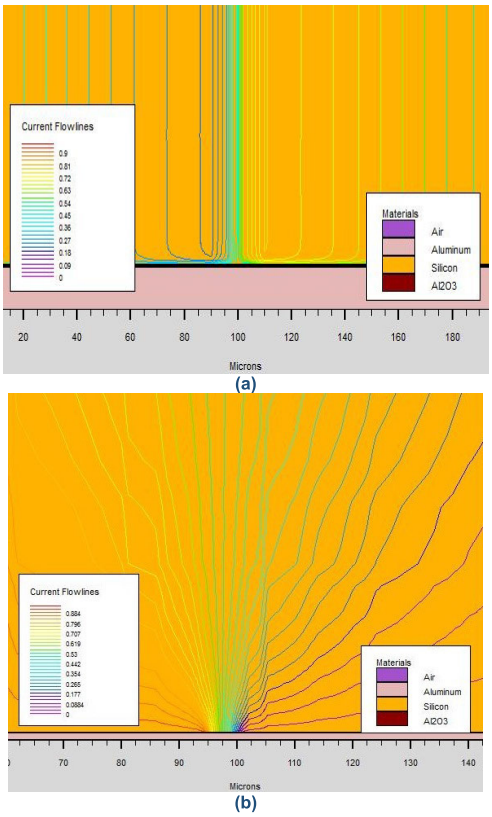


**FIGURE 2. Current flow lines for (a) 2 nm thick oxide layer with full area contact structure and (b) 20 nm thick oxide considering single localized area contact structure.**

Larger the ratio, smaller is the passivated surface area, which results in more recombination of carriers at the interface. Drop of $V_{OC}$ is also due to the higher contact recombination for larger value of $R$ as shown in Fig. 3(b).

It is evident from both the figures that result variation of $R$ is better for lower doping concentration of the substrate. Fill-factor is found to increase with the ratio for a particular doping concentration and does not vary significantly with doping concentration, thus not shown here for the sake of clarity of the figure. Decrease of the fill-factor at lower contact to non-contact area ratio is ascribed due to the higher series resistance at contact area. Doping concentration of $p$-Si absorber also plays an important role in choosing ratio for improved efficiency. Variation of $\eta$ with the absorber doping concentration for different values of $R$ is shown in Fig. 3(c). It is seen that, efficiency reaches maxima at a particular doping concentration. This variation is mainly due to the effect of bulk and surface recombination, which depend on $R$ and doping concentration together. For Fig. 3, the $Si/Al_2O_3$ interface recombination velocities are kept constant at 10 cm/s. It is observed that the role of $R$ on the optimized absorber doping concentration is insignificant here. However, the effect of $R$ is explored further by varying the $Si/Al_2O_3$ interface recombination velocity and fixed oxide charge density ($Q_f$).

Variation of $J_{SC}$ and efficiency with $R$ for the different recombination velocities as 10 cm/s and 100 cm/s, keeping

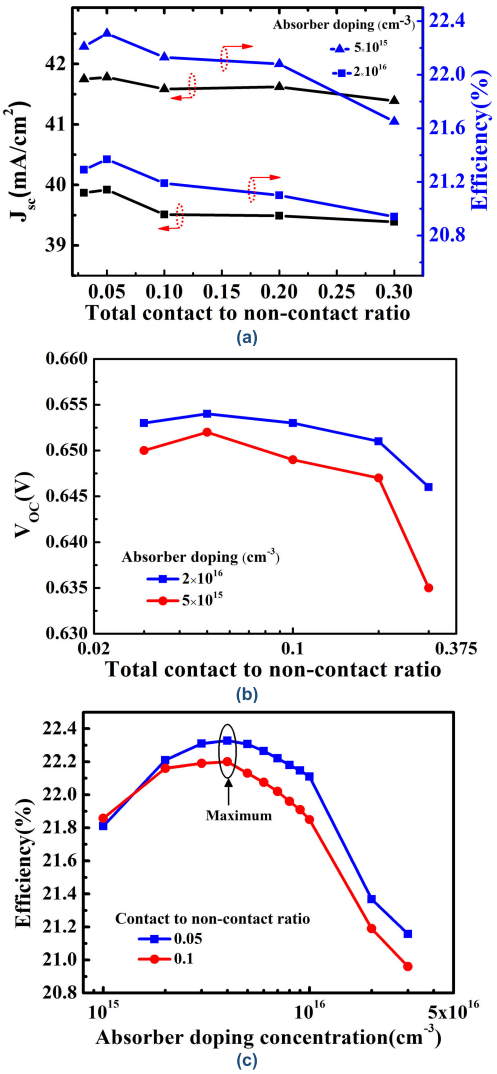


**FIGURE 3.** (a) Variation of $J_{SC}$ and $\eta$ with the ratio (R) between total area of localized contacts and area of non-contact surface for different absorber doping; (b) $V_{OC}$ vs ratio (R) characteristics for the same; (c) variation of $\eta$ with absorber doping concentration for different ratio (R) keeping the number of contact as one but to make different ratio, width of the contact is changed.

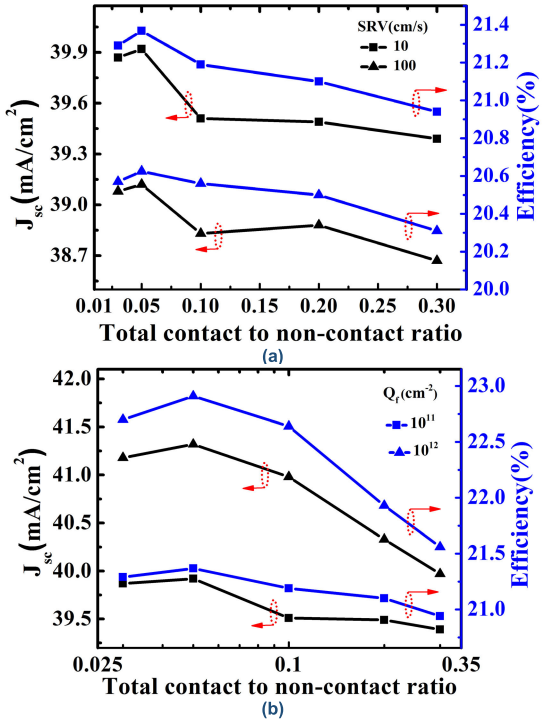


**FIGURE 4.** Variation of $J_{SC}$ and efficiency with ratio (R) for (a) different surface recombination velocities with fixed ve charge density ($Q_f$) = $10^{11}$ cm$^{-2}$ and (b) different fixed charge density values at Si/oxide interface. Charge densities are chosen based on the reported articles [29], [31], [32].

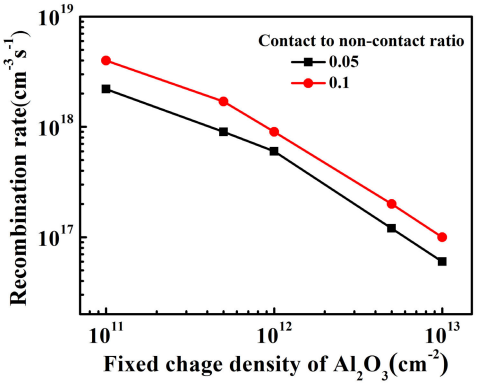


**FIGURE 5.** Variation of recombination rate with underlying fixed charge density of $Al_2O_3$ for different ratio of contact to non-contact area.

oxide charge density constant, is shown in Fig. 4(a). It is evident that effect of $R$ is significant for lower recombination velocities. Similar variation for two different values of underlying fixed charge density of $Al_2O_3$ as $10^{11}$ cm$^{-2}$ and $10^{12}$ cm$^{-2}$ is shown in Fig. 4(b). Values of fixed charge density are chosen based on their reported values [16], [28], [29]. However, the recombination velocities are not taken constant here. The recombination velocities are taken as 10 cm/s and 5 cm/s respectively for fixed charge density values of $10^{11}$ cm$^{-2}$ and $10^{12}$ cm$^{-2}$ [20]. It is observed from Fig. 4(b) that, choice of $R$ is important for higher oxide charge density, which yields better passivation and hence lower recombination.

Interface fixed charge density plays very important role in the surface passivation. The value of $Q_f$ may be varied based on the deposition technology and the growth kinetics under consideration. For instance, in case of thermal ALD, $Q_f$ value exhibited by $Al_2O_3$ film is in the order of $10^{11}$ cm$^{-2}$ whereas for plasma ALD, $Q_f$ value is in the order of $10^{12}$ cm$^{-2}$ which is also 'dependent on annealing temperature less than 400°C [20].

The effect of oxide fixed charge density on recombination rate is further explored and it is found that after increasing the oxide fixed charge density upto the experimental limit [20], [29], the recombination rate is reduced as shown in Fig. 5. This can be explained as the rate of recombination depends on both electron and hole concentration. Here, at the interface of absorber and $Al_2O_3$, built in electric field due to higher order negative fixed charge, repels the minority

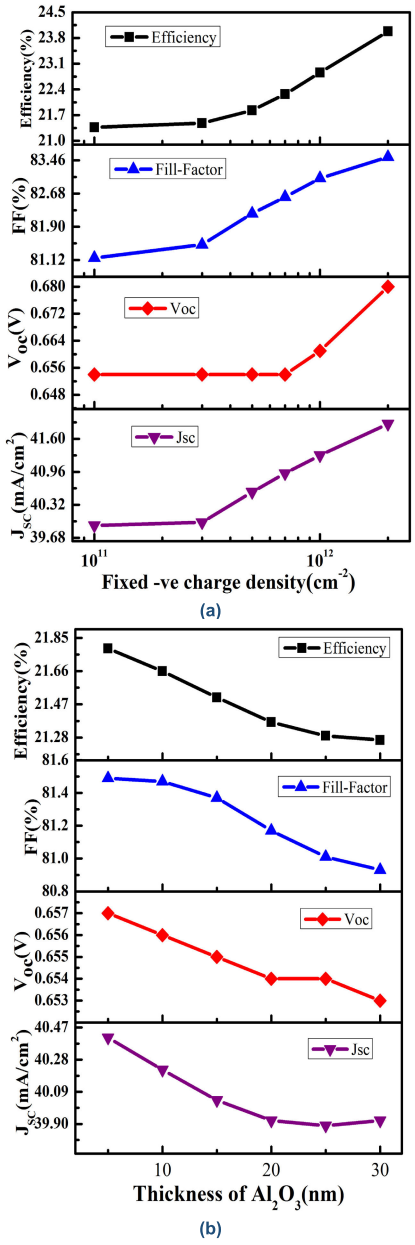


**FIGURE 6.** Performance parameters of the designed cell for (a) variation of ve fixed charge density of $Al_2O_3$ at Si/oxide interface and (b) variation of thickness of $Al_2O_3$. Charge densities are chosen based on the reported articles [31], [32].

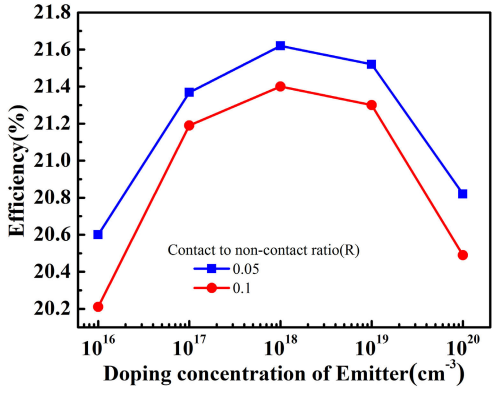


**FIGURE 7.** Variation of efficiency with different values of emitter doping concentration at different contact to non-contact ratio (R).

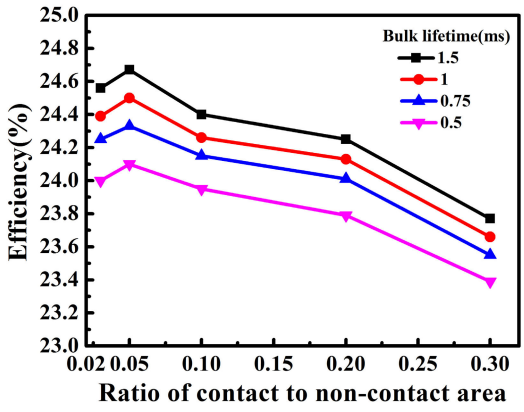


**FIGURE 8.** Representation of Efficiency at various bulk lifetime considering other parameters with their optimized values.

electrons from the oxide interface as mentioned in Fig. 1(c). This results the reduction in concentration of electron as well as the recombination rate at the interface. Also, the reduction of recombination due to higher fixed charges leads to the improvement of the device performances as shown in Fig. 6(a). Moreover, the value of electric field corresponding to the oxide fixed charge density of $1 \times 10^{11}$ $cm^{-2}$ and $2 \times 10^{12}$ $cm^{-2}$ are found to be $5.5 \times 10^4$ V/cm and $1.85 \times 10^5$ V/cm respectively. It signifies that the higher fixed charge density creates higher electric field at the $Si/Al_2O_3$ interface, which is responsible for stronger repulsion of the minority electrons and results in lowering the recombination through the reduction of effective capture length at interface. Thus, the field effect passivation is effective in this case. Moreover, due to the excellent field-effect passivation caused by the high negative fixed charge density at the c-$Si/Al_2O_3$ interface, interface recombination is also suppressed [33].

Now the effect of thickness of the $Al_2O_3$ on the device performance has also been studied to observe the passivation effect of designed cell. Selected range of thickness can be deposited by plasma assisted ALD or thermal ALD by choosing process parameters such as number of cycles restricted within 300 at deposition temperature of 250°C [20]. It is evident that performance parameters deteriorate for higher thickness of oxide passivation layer as found in Fig. 6(b). It may be attributed due to the fact that, thin oxide layer produces stronger electric field at the interface due to its underlying fixed charges compared to its thicker counterpart. However, it is not recommended to use the oxide thickness below 10 nm in order to maintain the industrial process feasibility since, oxide defects increases below this thickness [34], [35].

Doping concentration of *n*-Si emitter also plays an important role to get optimized cell performance, since minority carrier lifetime is proportional to diffusion length which is dependent on doping concentration. For heavily doped emitter, diffusion length is reduced which enables carrier

recombination before it reaches to top contact. However, for lower doping level, internal series resistance increases. It is well evident that optimum efficiency is found at the emitter doping level of $1 \times 10^{18}$ cm$^{-3}$ as shown in Fig. 7 and degrades below and afterwards due to the said reasons.

Improved efficiency with the optimized values of cell parameters under study is plotted in Fig. 8 with different lifetimes. It is notable that reported highest efficiency (24.06%) PERC cell uses lifetime higher than 1.5 ms but the wafer is costly to fabricate [16], [35], [36]. Our optimized cell shows improved efficiency of 24.67% with lifetime as 1.5 ms. Even with relatively lower lifetime of 1 ms. an enhanced efficiency of 24.5% with higher $V_{OC}$ ∼700 mV can be achieved considering the rear contact to non-contact area ratio as 0.05 with fixed charge density of $-2 \times 10^{12}$ cm$^{-2}$ for a 10-20 nm thick $Al_2O_3$ passivating layer at rear side of the illustrated cell including optimized doping concentration of both emitter and base.

## IV. CONCLUSION

Enhancement of efficiency through analytical modeling of *p*-Si solar cell having lower lifetime compared to state of art PERC cell is outlined. However, for obtaining significant improvement, proper design of the device, mainly in terms of ratio between localized contact and non-contact surface area, fixed charge density of passivated layer and carrier concentrations in both the emitter and base layers are required. Some best possible designs for rear-surface passivated *p*-Si solar cell with localized contact is proposed. Area of the rear contact coverage should be as low as ∼5% of the rear surface area whereas doping concentration of absorber and emitter should be chosen in the order of $4 \times 10^{15}$ cm$^{-3}$ and $1 \times 10^{18}$ cm$^{-3}$ respectively in order to obtain improved efficiency of the device. An enhanced efficiency of 24.5% with high $V_{OC}$ of ∼700 mV can be achieved using *p*-Si wafer even with relatively low carrier-lifetime, by maintaining the rear contact to non-contact area ratio as ∼0.05 and fixed charge density as -2 × $10^{12}$ cm$^{-2}$ for a 10-20 nm thick $Al_2O_3$ passivating layer which is quiet feasible to grow.

## REFERENCES


[1] S. Gatz, T. Dullweber, and R. Brendel, "Evaluation of series resistance losses in screen-printed solar cells with local rear contacts," *IEEE J. Photovolt.*, vol. 1, no. 1, pp. 37–42, Jul. 2011, doi: 10.1109/JPHOTOV.2011.2163925.

[2] T. Lauermann, T. Lüder, S. Scholz, B. Raabe, G. Hahn, and B. Terheiden, "Enabling dielectric rear side passivation for industrial mass production by developing lean printing-based solar cell processes," in *Proc. 35th IEEE Photovoltaic Spec. Conf. (PVSC)*, Honolulu, HI, USA, Jun. 2010, pp. 28–33.

[3] A. W. Blakers, A. Wang, A. M. Milne, J. Zhao, and M. A. Green, "22.8% efficient silicon solar cell," *Appl. Phys. Lett.*, vol. 55, no. 13, pp. 1363–1365, Sep. 1989, doi: 10.1063/1.101596.

[4] S. Mitra, H. Ghosh, H. Saha, and K. Ghosh, "Recombination analysis of tunnel oxide passivated contact solar cells," *IEEE Trans. Electron Devices*, vol. 66, no. 3, pp. 1368–1376, Mar. 2019, doi: 10.1109/TED.2018.2890584.

[5] W. Liang, K. J. Weber, and A. F. Thomson, "Effective $SiN_x$: H capping layers on 1-nm $Al_2O_3$ for $p^+$ surface passivation," *IEEE J. Photovolt.*, vol. 4, no. 6, pp. 1405–1413, Aug. 2014, doi: 10.1109/JPHOTOV.2014.2344757.

[6] A. Rohatgi, "Fabrication and modeling of high-efficiency front junction n-type silicon solar cells with tunnel oxide passivating back contact," *IEEE J. Photovolt.*, vol. 7, no. 5, pp. 1236–1243, Sep. 2017, doi: 10.1109/JPHOTOV.2017.2715720.

[7] J. Wang, S. S. Mottaghian, and M. F. Baroughi, "Passivation properties of atomic-layer-deposited hafnium and aluminum oxides on Si surfaces," *IEEE Trans. Electron Devices*, vol. 59, no. 2, pp. 342–348, Feb. 2012, doi: 10.1109/TED.2011.2176943.

[8] G. Dingemans, M. C. M. Van de Sanden, and W. M. M. Kessels, "Influence of the deposition temperature on the c-Si surface passivation by $Al_2O_3$ films synthesized by ALD and PECVD," *Electrochem. Solid State Lett.*, vol. 13, no. 3, pp. H76–H79, Jan. 2010, doi: 10.1149/1.3276040.

[9] M. H. Kang, Y.-W. Ok, and A. Rohatgi, "Investigation of atomic layer deposition $Al_2O_3$ passivation for screen-printed large-area solar cells," *IEEE J. Photovolt.*, vol. 6, no. 4, pp. 869–874, Jul. 2016, doi: 10.1109/JPHOTOV.2016.2556982.

[10] Y.-P. Shen and J.-G. Hwu, "Metal oxide semiconductor solar cells with silicon dioxide prepared by liquid-phase deposition method," *IEEE Photon. Technol. Lett.*, vol. 8, no. 3, pp. 420–421, Mar. 1996, doi: 10.1109/68.481154.

[11] B. Vermang, A. Rothschild, A. Racz, J. John, J. Poortmans, R. Mertens, P. Poodt, V. Tiba, and F. Roozeboom, "Spatially separated atomic layer deposition of $Al_2O_3$, a new option for high-throughput Si solar cell passivation," *Prog. Photovolt., Res. Appl.*, vol. 19, no. 6, pp. 733–739, Feb. 2011, doi: 10.1002/pip.1092.

[12] P. Poodt, "Spatial atomic layer deposition: A route towards further industrialization of atomic layer deposition," *J. Vac. Sci. Technol. A*, vol. 30, no. 1, Jan. 2012, Art. no. 010802, doi: 10.1116/1.3670745.

[13] M. Rauer, "Aluminum alloying in local contact areas on dielectrically passivated rear surfaces of silicon solar cells," *IEEE Electron Device Lett.*, vol. 32, no. 7, pp. 916–918, Jun. 2011, doi: 10.1109/LED.2011.2143385.

[14] L. E. Black and K. R. McIntosh, "Surface passivation of c-Si by atmospheric pressure chemical vapor deposition of $Al_2O_3$," *Appl. Phys. Lett.*, vol. 100, no. 20, May 2012, Art. no. 202107, doi: 10.1063/1.4718596.

[15] T. Dullweber and J. Schmidt, "Industrial silicon solar cells applying the passivated emitter and rear cell (PERC) concept—A review," *IEEE J. Photovolt.*, vol. 6, no. 5, pp. 1366–1381, Sep. 2016, doi: 10.1109/JPHOTOV.2016.2571627.

[16] F. Jianbin, "The roadmap to >24% PERC," in *Proc. 29th Int. PV Sci. Eng. Conf. (PVSEC)*, Xi'an, China, Nov. 2019, pp. 1–13.

[17] X. Cai, X. Zhou, Z. Liu, F. Jiang, and Q. Yu, "An in-depth analysis of the silicon solar cell key parameters' optimal magnitudes using PC1D simulations," *Optik*, vol. 164, pp. 105–113, Jul. 2018, doi: 10.1016/j.ijleo.2018.02.102.

[18] H. Mehmood and T. Tauqeer, "Modelling and performance analysis of amorphous silicon solar cell using wide band gap nc-Si: H window layer," *IET Circuits, Devices Syst.*, vol. 11, no. 6, pp. 666–675, Nov. 2017, doi: 10.1049/iet-cds.2017.0072.

[19] W. Shockley and W. T. Read Jr., "Statistics of the recombinations of holes and electrons," *Phys. Rev.*, vol. 87, pp. 835–842, Sep. 1952, doi: 10.1103/PhysRev.87.835.

[20] G. Dingemans and W. M. M. Kessels, "Status and prospects of $Al_2O_3$-based surface passivation schemes for silicon solar cells," *J. Vac. Sci. Technol. A*, vol. 30, no. 4, Jul. 2012, Art. no. 040802, doi: 10.1116/1.4728205.

[21] P. Calado, I. Gelmetti, B. Hilton, M. Azzouzi, J. Nelson, and P. R. F. Barnes, "Driftfusion: An open source code for simulating ordered semiconductor devices with mixed ionic-electronic conducting materials in one dimension," *J. Comput. Electron.*, vol. 21, no. 4, pp. 960–991, Aug. 2022, doi: 10.1007/s10825-021-01827-z.

[22] A. Rohatgi and P. Rai-Choudhury, "Design, fabrication, and analysis of 17–18% efficient surface-passivated silicon solar cells," *IEEE Trans. Electron Devices*, vol. ED-31, no. 5, pp. 596–601, May 1984, doi: 10.1109/T-ED.1984.21574.

[23] N. Balaji, D. Lai, V. Shanmugam, P. K. Basu, A. Khanna, S. Duttagupta, and A. G. Aberle, "Pathways for efficiency improvements of industrial PERC silicon solar cells," *Sol. Energy*, vol. 214, pp. 101–109, Jan. 2021, doi: 10.1016/j.solener.2020.11.025.

[24] J. W. Lin, Y.-Y. Chen, J.-Y. Gan, W.-P. Hseih, C.-H. Du, and T.-S. Chao, "Improved rear-side passivation by atomic layer deposition $Al_2O_3/SiN_x$ stack layers for high VOC industrial p-type silicon solar cells," *IEEE Electron Device Lett.*, vol. 34, no. 9, pp. 1163–1165, Jul. 2013, doi: 10.1109/LED.2013.2271894.

[25] A. Augusto, A. Srinivasa, R. R. King, and S. G. Bowden, "Performance of silicon heterojunction solar cells using high resistivity substrates," in *Proc. IEEE 46th Photovoltaic Spec. Conf. (PVSC)*, Jun. 2019, pp. 0300–0303, doi: 10.1109/PVSC40753.2019.8981236.
[26] A. K. W. Chee, "Principles of high-resolution dopant profiling in the scanning helium ion microscope, image widths, and surface band bending," *IEEE Trans. Electron Devices*, vol. 66, no. 11, pp. 4883–4887, Nov. 2019, doi: 10.1109/TED.2019.2940562.
[27] A. K. W. Chee, R. F. Broom, C. J. Humphreys, and E. G. T. Bosch, "A quantitative model for doping contrast in the scanning electron microscope using calculated potential distributions and Monte Carlo simulations," *J. App. Phys.*, vol. 109, pp. 013109-1–013109-10, Jan. 2011, doi: 10.1063/1.3524186.
[28] B. Hoex, J. Schmidt, P. Pohl, M. C. M. van de Sanden, and W. M. M. Kessels, "Silicon surface passivation by atomic layer deposited $Al_2O_3$," *J. Appl. Phys.*, vol. 104, no. 4, Aug. 2008, Art. no. 044903, doi: 10.1063/1.2963707.
[29] X. Wang and Z. M. Wan, *High-Efficiency Solar Cells Physics, Materials, and Devices* (Springer Series in Materials Science) vol. 190. London, U.K.: Springer, 2014, pp. 15–21, doi: 10.1007/978-3-319-01988-8.
[30] A. Fell, K. R. McIntosh, P. P. Altermatt, G. J. M. Janssen, R. Stangl, A. Ho-Baillie, H. Steinkemper, J. Greulich, M. M'uller, B. Min, K. C. Fong, M. Hermle, I. G. Romijn, and M. D. Abbott, "Input parameters for the simulation of silicon solar cells in 2014," *IEEE J. Photovolt.*, vol. 5, no. 4, pp. 1250–1263, Jul. 2015, doi: 10.1109/JPHOTOV.2015.2430016.
[31] G. Dingemans, "Influence of the oxidant on the chemical and field-effect passivation of Si by ALD $Al_2O_3$," *Electrochemical Solid-State Lett.*, vol. 14, no. 1, p. H1, 2011, doi: 10.1149/1.3501970.
[32] F. Werner, B. Veith, V. Tiba, P. Poodt, F. Roozeboom, R. Brendel, and J. Schmidt, "Very low surface recombination velocities on p- and n-type c-Si by ultrafast spatial atomic layer deposition of aluminum oxide," *Appl. Phys. Lett.*, vol. 97, no. 16, Oct. 2010, Art. no. 162103, doi: 10.1063/1.3505311.
[33] F. Werner, A. Cosceev, and J. Schmidt, "Silicon surface passivation by $Al_2O_3$: Recombination parameters and inversion layer solar cells," *Energy Proc.*, vol. 27, Apr. 2012, pp. 319–324.
[34] F. Werner, B. Veith, D. Zielke, L. Kühnemund, C. Tegenkamp, M. Seibt, R. Brendel, and J. Schmidt, "Electronic and chemical properties of the c-Si/$Al_2O_3$ interface," *J. Appl. Phys.*, vol. 109, no. 11, Jun. 2011, Art. no. 113701, doi: 10.1063/1.3587227.
[35] S. Banerjee and M. K. Das, "A review of $Al_2O_3$ as surface passivation material with relevant process technologies on c-Si solar cell," *Opt. Quantum Electron.*, vol. 53, no. 1, pp. 1–25, Jan. 2021, doi: 10.1007/s11082-020-02689-8.
[36] M. Osborne. (2019). *LONGi Solar has Bifacial Mono-PERC Solar Cell World Record Verified at 24.06%*. Accessed: Jan. 1, 2023. [Online]. Available: https://www.pv-tech.org/news/longi-solar-has-bifacial-mono-perc-solar-cell-world-record-verified-at-24.0

**S. BANERJEE** received the B.Tech. degree in Electronics and Communication Engineering from the Kalyani Government Engineering College, West Bengal, India, in 2007, and the M.Tech. degree from the Indian Institute of Technology Kharagpur, India, in 2013. He is currently pursuing the Ph.D. degree from the Department of Electronics Engineering, Indian Institute of Technology (Indian School of Mines) Dhanbad, India.

He was a Research Project Assistant with the Central Mechanical Engineering Research Institute (CMERI), Durgapur, India, from 2009 to 2010. He has been a faculty member of different Engineering colleges in West Bengal, since 2010. He has been an Assistant Professor with the Department of Electronics and Communication Engineering, NSHM Institute of Engineering and Technology, NSHM Knowledge Campus, Durgapur, since 2015. His current research interests include modeling and analysis of solar cells. He was a recipient of the Best Paper Award from the National Conference on Science Technology and Management, India, in 2022.

**S. S. A. ASKARI** (Member, IEEE) received the B.Tech. degree in Electronics and Communication Engineering from the West Bengal University of Technology, Kolkata, India, in 2010, the M.Tech. degree in Electronics and Communication Engineering from IIT(ISM) Dhanbad, India, in 2012, and the Ph.D. degree in photovoltaics from the Department of Electronics Engineering, IIT(ISM) Dhanbad, in 2021.

He was a Junior Research Fellow with the Department of Electronics and Electrical Communication Engineering, IIT, Kharagpur, India, from 2013 to 2014. He was a Research Associate with the Centre of Excellence in Renewable Energy, IIT(ISM) Dhanbad, from 2019 to 2021. He is currently a Research Associate with the Department of Electronics Engineering, IIT(ISM) Dhanbad. His current research interests include the modeling of the spectral response of quantum dot solar cells, simulation and PVD growth of complete oxide-based thin-film solar cells, and metal-oxide semiconductor-based thin-film solar cells. He served as an active member for various technical and professional societies, such as OSA and SPIE. He is a Life Fellow of the Optical Society of India (OSI) and a Life Member of the Solar Energy Society of India (SESI). He was a recipient of the M.H.R.D. Scholarship for master's and Ph.D. studies. He served as the Vice-President for the SPIE Student Chapter and OSA Student Chapter ISM. He served as a Reviewer for journals, such as the IEEE Journal of Photovoltaics, *Semiconductor Science and Technology* (IOP), *Engineering Research Express* (IOP), *Nano Express* (IOP), *IET Micro and Nano Letters*, and *The European Physical Journal Applied Physics*.

**M. K. DAS** (Senior Member, IEEE) received the B.Tech. and M.Tech. degrees in Radio Physics and Electronics from the University of Calcutta, in 1998 and 2000, respectively, and the Ph.D. (Tech.) degree from the Institute of Radio Physics and Electronics, University of Calcutta, in 2008.

He was a full-time Faculty Member with the A. K. Choudhry School of Information Technology, University of Calcutta, during the Ph.D. degree. He was a Faculty Member of different Engineering colleges in West Bengal, India, from 2000 to 2004. He was an Internship Research Fellow with Ecole Polytechnic, France, from June 2008 to August 2008. He was a Faculty Fellow with the University of Calcutta, in 2008. He joined IIT(ISM) Dhanbad, Dhanbad, Jharkhand, India, in September 2008. He is currently an Associate Professor with the Department of Electronics Engineering, IIT(ISM) Dhanbad. He is also the Head and a Project Coordinator with the Centre of Excellence in Renewable Energy, under FAST, MHRD, Government of India. He has published more than 25 research articles in SCI international journals and guided seven Ph.D. students to date. His research interests include the design and development of solar photovoltaic devices, modeling of Gr-IV-based optoelectronic devices, and growth and study of metal oxide semiconductor-based thin films by the physical vapor deposition technique.

Dr. Das was a recipient of the Young Scientist Award by the International Union of Radio Science (URSI) in its General Assembly held in Chicago, IL, USA, in 2008. He was also a recipient of the National Scholarship for B.Sc. (Hons.) and was awarded by the Indian Association of Physics Teachers for qualifying for Part A and Part B of the National Graduate Physics Examination (NGPE), in 1995.